Redox-active cerium oxide based nanozyme abrogate the organophosphate mediated poisoning in mammalian cells

Kinjal D. Shah, Ragini Singh, Sanjay Singh*

Division of Biological and Life Sciences, School of Arts and Science, Central Campus, Ahmedabad University, Navrangpura, Ahmedabad 380009, Gujarat, India

*Corresponding author

DOI: 10.5185/amlett.2018.1939
www.vbripress.com/aml

Abstract

Owing to the autocatalytic antioxidant activity, cerium oxide nanoparticle (CeNPs) has been extensively used in biomedical fields for treatment of neurodegenerative diseases, biosensing, and therapeutic applications. The redox-dependent interconversion between +3 and +4 oxidation states of CeNPs is suggested to be the reason of scavenging of free radical generated in the biological system. Herein we have explored the protective effect of CeNPs against the oxidative stress induced by organophosphate-based pesticide, 2,2-dichlorovinyl dimethyl phosphate (DDVP), in a normal human liver cell culture model (WRL-68). DDVP is known to cause the toxic effect in cells by inducing lipid peroxidation, cellular glutathione level depletion and DNA fragmentation by the caspase-dependent pathway. We followed the protection of cells by CeNPs against DDVP exposure using MTT and NRU assays. Exposure of DDVP to cells induced significant nuclear fragmentation, which could be avoided in cells pre-treated with CeNPs. Mechanistically, we observed that CeNPs induces an increase in cellular GSH level, which could assist in removal of excess of reactive oxygen species, generated in DDVP exposed cells, along with the superoxide dismutase (SOD)-like activity of CeNPs. The interaction study showed that there was no chemical interaction between DDVP and CeNPs, therefore, the intrinsic SOD-like activity of CeNPs was intact even in the complex cell culture media. Growing evidence suggest that excess use of DDVP could lead to the several diseases in cells/tissues, therefore our finding emphasizes that CeNPs can be used as a potent antioxidant agent to avoid the ramifications of DDVP and other commercial pesticides.

Keywords: Nanozymes, superoxide-dismutase, organophosphate, Dichlorvos Pesticide (DDVP), antioxidant nanoparticles, oxidative stress.

Introduction

Last few decades have seen the synthesis of a plethora of nanomaterials which are expected to be extensively used for potential applications in diagnostics, therapeutics and theranostics [1-4]. Among them, CeNPs have been recently discovered as a potent therapeutic agent due to its redox activity-dependent antioxidant nature [5]. The ability of CeNPs to switch its oxidation state between +3 and +4 oxidation state offers autocatalytic behavior, which renders them as an exceptional inorganic antioxidant [6]. It is argued that CeNPs possess antioxidant activity due to surface oxygen vacancy/defect in their crystal structure which facilitates the interconversion of +3 and +4 oxidation states [7, 8]. Self and co-workers have reported that the oxidation state switching properties of "Ce" atoms is responsible for the biological enzyme mimetic activities of CeNPs [9-12]. CeNPs with high +3 oxidation state "Ce" atoms exhibit the activity of naturally occurring superoxide dismutase enzyme whereas CeNPs with high +4 oxidation states mimics the biological catalase enzyme-like activity [11-14]. It has also been reported that once internalized in mammalian cells, CeNPs are almost uniformly distributed in the cell cytoplasm and also in multiple compartments of the cell, suggesting that recent efficacy of CeNPs as an antioxidant may be partly due to this widespread distribution [15]. The protective effect of CeNPs against reactive oxygen (ROS) and nitrogen (RNS) species have found their applications in the treatment of various neurodegenerative disorders and diseases triggered by free radicals [16]. Several reports dealing with free radical scavenging properties of CeNPs have been tested in various cell cultures such as skin, breast, endothelial, gastrointestinal and neuronal cell lines and animal models and shown positive results [17-19].

Acute poisoning with agricultural pesticides has been a global health problem for several decades. Among them, organophosphates, such as DDVP, methyl parathion, chlorpyrifos are the most commonly used pesticides that are known to induce serious health issues, particularly neurodegenerative diseases [20, 21]. It has been reported that DDVP exposure to neuronal cell

culture model cell line PC 12 has resulted in free radical-mediated DNA damage along with activation of cell cycle machinery [22]. The general mechanism of pesticide-mediated toxicity is enhanced lipid peroxidation, reduced glutathione levels with concomitant increase in oxidative stress. DDVP is also reported to be a potent inhibitor of acetylcholinesterase (AChE) in insects and in human [23-25]. Acetylcholinesterase is an important enzyme for efficient neuronal functionalization [26]. DDVP is commercially available organophosphate which has known to cause acute and chronic toxicity and used for insect and parasite control [27, 28]. Studies have shown that DDVP severely affects the neuromuscular and parasympathetic autonomic nervous system, as well as non-neuronal targets like human plasma, kidney, liver, and reproductive system [27]. It was already reported that DDVP caused DNA damage in HCT116 cell lines via caspase-dependent pathway which leads to cell death [26]. Its toxicity is also reported in different cell culture models of other organs as well [29, 30]. The liver is the primary site for detoxification of DDVP by converting it into less toxic dimethyl phosphate. In liver cells, DDVP is reported to induce hepatocellular vacuoles and cell swelling [31]. DDVP has been found to mostly modify the serine in the active sites of cholinesterases, however, also forms adducts with unrelated targets such as transferrin and albumin thereby cause perturbations in cellular processes by altering non-cholinesterase targets and inhibits the activity of key enzymes [27]. Although several antioxidant treatments have shown protective effects against the cytotoxicity induced by DDVP, however the non-specific modification of biological enzymes remains the major bottleneck in the effective abrogation of DDVP-incited toxicity.

In this context, we report here the use of redox-active CeNPs to protect the normal liver cell culture model (WRL-68) against the toxicity generated by DDVP. It was observed that the exposure of CeNPs to cells treated with DDVP undergo high expression of glutathione (GSH), which is expected to play a significant role, along with CeNPs, towards the protection of cells against generated free radicals. Unlike the non-specific interaction of DDVP with biomolecules present in mammalian cells, it did not show any interaction with inorganic CeNPs. To best of our knowledge, this is the first report to show the redox active CeNPs mediated protection of WRL-68 cells against the DDVP mediated oxidative stress.

Materials and experimental methods

Materials

Cerium nitrate hexahydrate, 2, 7- dichloroflourescin diacetate (H_2DCFDA), ferricytochrome C, xanthine oxidase and catalase were purchased from Sigma Aldrich (St. Louis, MO, USA). Hydrogen peroxide was obtained from SD Fine Chemical Limited (Mumbai, India). Hypoxanthine, Potassium bromide (KBr), 3-(4,5-dimethylthiazol-2-yl)-2,5-diphenyltetrazolium bromide (MTT) dye, neutral red dye, phosphate Buffered Saline (PBS), 4'6-diamidino-2-phenylindole (DAPI), Tris-hydrochloride and Minimum Essential Medium were purchased from Hi-Media Pvt. Ltd. (Mumbai, India). Dichlorvos (dichlorovinyl dimethyl phosphate-DDVP) was purchased from local market.

Synthesis of cerium oxide nanoparticles

CeNPs were synthesized by the method described by Karakoti et al [32]. In brief, 0.1 gm cerium nitrate hexahydrate was dissolved in 49 ml deionized water and upon addition of 1 ml 30% H_2O_2 , the colourless solution turns into yellow colour, indicating the formation of CeNPs with high +4/+3 oxidation state. Gradually in 10-15 days, the yellow colour solution turns colourless indicating the formation of CeNPs with high +3/+4 state. This transition was also monitored using UV-visible spectrophotometer (Biotek, Synergy HT spectrophotometer).

UV-visible spectroscopy analysis

CeNPs were suspended in water along with different DDVP concentrations (100 to 1000 µM) and the resulting suspensions were analysed using UV-visible spectroscopy. CeNPs, DDVP and a mixture of CeNPs and DDVP were treated with 1M H_2O_2 for 1 hr followed by UV-visible spectra measurements.

Zeta potential measurements

CeNPs were suspended in complete and incomplete culture medium (Minimal Essential Medium) followed by charge measurements by Zeta Sizer Nano (Malvern Instruments) using a laser of wavelength at 633 nm.

SOD activity-like measurement

SOD mimetic activity of CeNPs was measured by the method reported by Korsvik et al [13]. In brief, the competition for reduction of ferricytochrome C by superoxide radicals was measured by increasing absorbance at 550 nm using UV-visible spectrophotometer. The superoxide radicals were generated by hypoxanthine and xanthine oxidase in a reaction system. Catalase was added to avoid interference of H_2O_2 in the system. The reactions were carried out in 96 well plate in triplicates with a total volume of 100 µl for 20 mins and buffered with 10 mM Tris pH 7.5.

Fourier Transform Infrared Spectroscopy (FTIR)

The samples (CeNPs, DDVP and a mixture of CeNPs and DDVP) were dried for some time, crushed, prepared in KBr powder and analysed using the ATR mode from in 400 – 4000 cm^{-1} range using Spectrum Two FT-IR Spectrometer, L160000A, PerkinElmer.

Transmission Electron Microscopy (TEM)

Sample was prepared by adding drop of CeNPs on a carbon coated copper grid. After drying, images were acquired by transmission electron microscopy (TEM), JEOL JEM 1400 operating at a voltage of 120 kV.

Cell culture and exposure of WRL-68 cells to CeNPs

Human normal liver cell line (WRL-68), purchased from the national cell culture repository situated in National Centre for Cell Sciences (NCCS), Pune, India was cultured in Minimal Essential Medium (MEM) supplemented with 10% FBS and 1% antibiotic - antimycotic solution at 37^0C under a humidified atmosphere of 5% CO_2. Stock solutions of CeNPs (1mM) were prepared in MEM (supplemented with 10% FBS) was serially diluted to concentrations (50 µM) for cellular uptake, cytotoxicity assays, ROS generation and oxidative stress parameters. The experiments were performed between the passage no. 34 - 48 for WRL-68 cells. For experiments involving DDVP treatment, cells were pre-incubated with CeNPs for 6 hrs followed by 18 hrs of DDVP treatment.

Cellular uptake of CeNPs

Internalization of CeNPs was analysed by flow cytometry as described by Suzuki *et al* [33]. $1x10^5$ cells were seeded in a 6-well cell culture plate and allowed to grow overnight. Cells were treated with a fixed concentration of CeNPs (50 µM) for 3, 6, 8 and 24 hrs. After exposure, cells were harvested by trypsinization and washed with PBS. Finally the cell pellet were suspended in PBS and the uptake of particles was analysed by flow cytometer (FACS Calibur, BD Biosciences, CA) with side scatter intensity (SSC). For fold change, SSC intensity values of treated cells were divided by SSC value of control (untreated) cells.

Cytotoxicity assessment

MTT assay was done to evaluate the mitochondrial activity by protocol as described by Mosmann *et al* [34]. $1x10^4$ cells were seeded in 96-well cell culture plates and allowed to grow overnight. Cells were pre-incubated with CeNPs (50 µM) for 6 hrs, followed by DDVP (100, 200 µM) treatment for 18 hrs. The MTT (0.5 mg/ml) dye was added to the plate and incubated at 37^0C for 3 hrs. The resulting formazan crystals were solubilized by adding 200µl of dimethyl sulphoxide (DMSO) and quantified by measuring absorbance at 590nm in a multiwell plate reader (Biotek, Synergy HT spectrophotometer).

Neutral Red Uptake (NRU) assay

Viability of cells was also assessed by neutral red uptake assay which accumulate in the lysosomes of viable cells. $1x10^4$ cells were seeded in 96 well cell culture plates and allowed to grow overnight. Cells were pre-incubated with CeNPs (50 µM) for 6 hrs, followed by DDVP (100, 200 µM) treatment for 18 hrs. The neutral red (40 µg/ml) was prepared in the serum-free medium and added to each well after discarding the media. The plate was incubated for 3 hrs at 37^0C and the accumulated dye was dissolved in destaining solution (50% ethanol, 49% deionized water and 1% glacial acetic acid), followed by absorbance at 540 nm in a multiwell plate reader.

Glutathione estimation

Free sulphydryl content was measured with Glutathione estimation kit (Cayman) and expressed as µmole/mg of protein. In brief, $1x10^5$ cells were seeded in a 6 well cell culture plate and incubated for 24 hrs. Cells were pre-incubated with CeNPs (50 µM) for 6 hrs followed by DDVP treatment (100 µM) for 18 hrs. Cells were harvested by scrapper and sonicated in a cold buffer containing EDTA, centrifuged and supernatant was collected for further quantification. Supernatant was added into 96 well plate followed by the addition of reagent mixture provided in the kit. The plate was incubated in the dark for 15-20 mins at room temperature, followed by absorbance at 405 nm in a multiwell plate reader.

Reactive oxygen species level measurement

The level of intracellular ROS generation was determined by using 2, 7-dichloroflourescin diacetate dye. Here, higher level of peroxides were induced by DDVP treatment (100, 200 µM). $1x10^4$ cells were seeded in a 96 well black bottom cell culture plates and allowed to grow overnight. After 24 hrs, the cells were pre-incubated with CeNPs for 6 hrs followed by exposure of 100 and 200 µM DDVP for 18 hrs. The nanoparticle containing medium was aspirated, and cells were washed twice with 1X PBS. Thereafter, DCFDA (20 µM) dye was added to each and incubated at 37^0C for 30 mins. The dye was then discarded and 200 µl PBS was added to each well, followed by measurement of fluorescent intensity in a multiwell plate reader at excitation and emission wavelengths of 485 and 528 nm respectively. For qualitative analysis of ROS level generated in cells after DDVP exposure, imaging of cells under fluorescent microscope was used. Prior to imaging, cells were incubated with DCFDA dye for 30 mins, followed by cell-fixation with chilled (-20^0C) methanol for 10 mins. The cells were then incubated with DAPI for 10 mins, washed, mounted in anti-fade mounting agent (Calbiochem), and slides were prepared. These slides were stored at 0^0C until fluorescent imaging by DM 2500, Leica, (Wetzlar, Germany) with 40X objective lens.

Nuclear fragmentation

Fragmentation of the nucleus in DDVP treated WRL-68 cells were analysed by DAPI staining, which was further imaged by fluorescence microscope. Cells were seeded on a coverslip in a 12-well plate and incubated for 24 hrs. Cells were pre-incubated with 50 µM CeNPs, followed by 100 and 200 µM DDVP exposure for 18 hrs. The cells were washed with 1X PBS and stained with DAPI for 5-10 mins post-treatment. To remove any background stain, cover slips were gently washed with 1X PBS, then mounted on the slide. Further analysis was done by using fluorescence microscopy. For quantitative data ~ 150 cells were counted for each treatment and control.

Result and discussion

Characterization of CeNPs

The size and shape of as-synthesized pristine CeNPs were examined by TEM imaging **(Fig. 1A).** The TEM image clearly reveals that the particles are of quasi-spherical shape with ~38 nm diameter (Figure 1A, inset). As shown in **Table 1**, the high zeta potential value (+35.33 ± 2.34 mV), of CeNPs dispersion suggest that these nanoparticles are colloidally stable. The close packing of nanoparticles in TEM images could be due to the solvent drying effect on TEM grid. Further, the UV-vis spectra **(Fig. 1B)** shows two absorbance, a sharp absorbance at ~ 254 nm and a broad absorbance between 280 to 320 nm, which could be respectively assigned to "Ce" +3 and "Ce" +4 oxidation states present on the surface "Ce" atoms in CeNPs. A typical CeNP can have both +3 and +4 oxidation states, however, the ratio can be varied, which dictates the enzyme-like properties of CeNPs. FTIR analysis **(Fig. 1C and D)** shows that the aqueous suspension of CeNPs have characteristic transmission bands of "Ce-O" vibration and stretching bands at 1384 and 560 cm^{-1}, respectively. The stability and activity of nanomaterials can be altered upon suspension in biologically relevant buffers. The components of the buffers predominantly control the biological responses exhibited by the nanomaterials dispersed in buffers and media. Formation of "protein corona" and alteration in the intrinsic properties of nanomaterials are some of the famous examples [35, 36]. Therefore, it was imperative that the stability of pristine CeNPs be examined in the cell culture media before performing any cell culture-based experiments. The colloidal stability of pristine CeNPs suspended in incomplete (without serum) and complete (with 10% serum) cell culture media was analyzed by zeta potential measurement by DLS **(Table 1).**

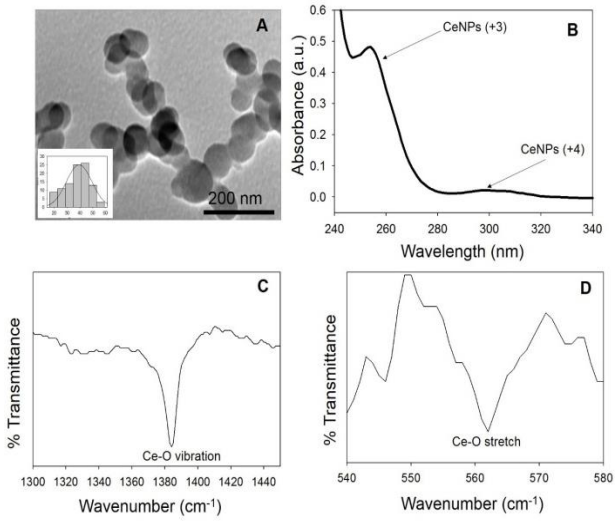

Fig. 1. Characterization of CeNPs. TEM images taken from as-prepared pristine CeNPs (A). The absorbance pattern of aqueous suspended CeNPs was recorded from UV-Visible spectrophotometer (B). Presence of characteristic transmission bands of Ce-O was examined by FTIR spectroscopy (C and D).

Table 1. Zeta potential values of CeNPs suspended in water, complete (with serum) and incomplete (without serum) cell culture media. Data expressed as SD calculated from three (n = 3) independent experiments.

Suspension Media	Zeta potential (mV)
Water	35.33 ± 2.34
Incomplete Minimum Essential Medium (MEM)	26.1 ± 1.46
Complete Minimum Essential Media (MEM)	3.20 ± 0.60

The results revealed that CeNPs suspended in incomplete media showed a slight decrease in zeta potential value (26.1 ± 1.46 mV), however nanoparticles suspended in complete media showed significant decrease (3.20 ± 0.60 mV) in zeta potential value. This decrease in the zeta potential value could be assigned due to the formation of protein corona over CeNPs surface. The complete cell culture media contains excess of (~10% serum) of proteins, and according to a study ~1% of protein present in suspension is enough to form a protein layer over the surface of suspended nanoparticles [37]. Further, the intrinsic SOD-like activity of CeNPs was also measured after suspending them in cell culture media (MEM) with or without serum proteins. As evident from figure ESI1, CeNPs suspended in water and incomplete media did not show any decrease in SOD-like activity. Interestingly, CeNPs suspended in complete media, despite of decrease in zeta potential values, also showed no appreciable decrease in SOD-like activity.

CeNPs are internalized in WRL-68 cells

In order to execute the antioxidant activity, it is expected that CeNPs must be actively internalized in mammalian cells. Therefore, we examined the uptake kinetics of CeNPs in a normal human liver cell culture model system (WRL-68 cells) by flow cytometer. A Flow cytometer is an extremely sensitive and powerful technique which can quantitatively estimate any alteration in the size as well as granularity of a mammalian cell by measuring the intensities of forward scattering (FSC) and side scattering (SSC), respectively [17]. Internalization of CeNPs is expected to increase the granularity of cytoplasm, which could lead to the increase in SSC intensity. **Fig. 2 (A – J)** clearly reveal that the uptake of CeNPs (50 µM) increases within the short period of time (3hr), whereas upon further exposure lead to the decrease in the internalization in WRL-68 cells. The gated region "R" represent the number of cells with increased SSC intensity. The results reveal that the increase in the number of cells with enhanced SSC intensity increases with time **(Fig. 2 B, D, F, H and J)** with respect to corresponding control **(Fig. 2 A, C, E, G** and **I).** A bar graph **(Fig. 2K)** representing the summary of CeNPs uptake kinetics show that the internalization increases (~1.6 fold) up to 3 hrs followed by little decrease, which remains almost constant up to 8 hrs. Further, the

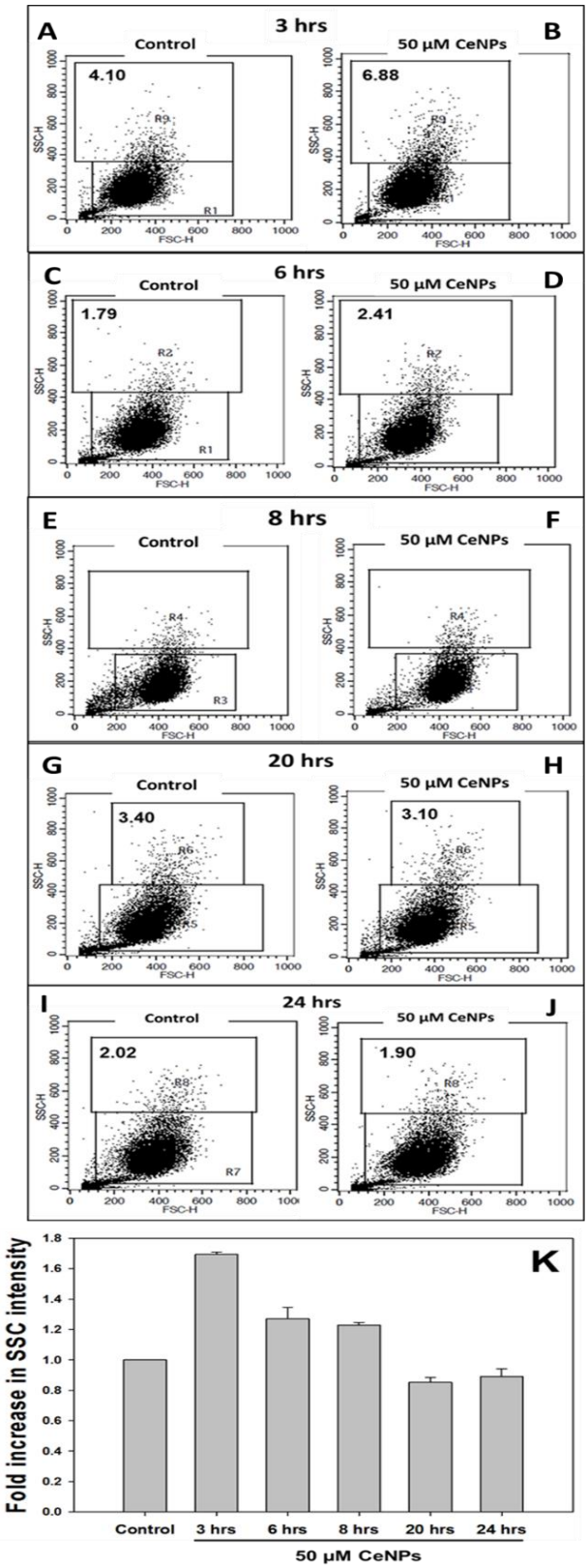

Fig. 2. CeNPs are efficiently internalized by WRL-68 cells. The kinetics (3, 6, 8, 20 and 24 hrs) of cellular internalization of pristine CeNPs was followed by flow cytometer. Figure A, C, E, G, I and B, D, F, H, I represents the cells unexposed and exposed to 50 µM CeNPs, respectively. The increase in SSC intensity due to CeNPs internalization at different time points has been plotted as fold uptake (K). Data expressed as standard deviation (SD) calculated from three (n = 3) independent experiments.

nanoparticle uptake was decreased when incubated for a longer period of time (24 hrs). This observation suggest that during initial periods of incubation cells rapidly internalize CeNPs, however after ~ 6 hrs cells may excrete out the excess of CeNPs and maintain an optimum amount. The obtained CeNPs uptake pattern lead us to fix the CeNPs pre-incubation time as 6 hrs before the cells are exposed to DDVP because the CeNPs concentration remains constant and optimum during these hours.

CeNPs show protection effect in WRL-68 cells against DDVP

DDVP is known to induce toxic effects on mammalian cells due to the generation of free radicals, which leads to the cell death. Therefore, in order to investigate the cytoprotective role of CeNPs against the toxicity generated by DDVP, we performed MTT and NRU assays in WRL-68 cells. In these experiments, WRL-68 cells were pre-incubated with CeNPs (50 µM) for 6 hrs before exposed with different concentrations (100 and 200 µM) of DDVP. As evident from MTT assay results **(Fig. 3A),** exposure of 100 and 200 µM of DDVP results in the decrease of cell viability to ~25 and 30%, respectively. However, WRL-68 cells pre-incubated with 50 µM CeNPs, showed the decrease in cytotoxicity effect induced by DDVP. As expected, pristine CeNPs alone did not induce any significant decrease in cell viability. MTT assay results indicated that CeNPs could circumvent the cytotoxicity induced by DDVP. To further confirm this, we performed NRU assay, which provides a quantitative estimate of the number of viable cells and it is considered as one of the best methods used in several biomedical and environmental applications [38]. Results revealed that exposure of 100 and 200 µM of DDVP to WRL-68 cells leads to decrease in cell viability to ~25% and 50%, respectively. However, cells pre-incubated with CeNPs resulted in only ~15% and 25% decrease in cell viability in presence of 100 µM and 200 µM concentration of DDVP. This observation is in accordance with our MTT data, thus suggest that about more than 50% of the cytotoxicity induced by DDVP can be abrogated by CeNPs. Similar to MTT assay, NRU results also showed that CeNPs alone does not exert any cytotoxicity to WRL-68 cells.

Exposure of CeNPs to WRL-68 cells modulate the production of GSH

GSH is well known cellular antioxidant present in high concentrations in the cell cytoplasm. It plays a significant role in maintaining the redox balance in the cytoplasm by controlling the ratio of reduced and oxidized GSH (GSH/GSSH). Lower ratio of GSH/GSSH is known to generate oxidative stress in cellular cytoplasm, which has been linked to the cause of neurodegenerative diseases. GSH protects the cells from oxidative stress induced by ROS and detoxifies superoxide anions and peroxides. Since, exposure of DDVP to mammalian cells also suggested to decrease the GSH level, we examined the level of cellular GSH

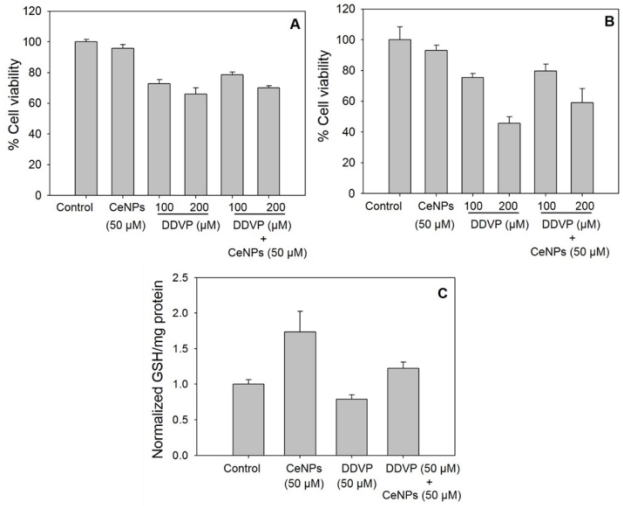

Fig. 3. CeNPs protect WRL-68 cells from DDVP induced cell death. Cell viability was examined by MTT (A) and NRU (B) assays after exposure of cells with 100 µM DDVP, with or without pre-treatment of 50 µM CeNPs for 6 hrs. Level of cellular GSH was measured from cells exposed to DDVP, with or without pre-treatment of CeNPs for 6 hrs (C). Data expressed as SD calculated from three (n = 3) independent experiments.

in cells pre-exposed to CeNPs and later exposed to DDVP. To our surprise, we observed that exposure of CeNPs to WRL-68 cells leads to the significant increase (~1.75 fold) increase in cellular GSH. However, Singh et al [17] have reported that exposure of PEGylated CeNPs alone to keratinocytic cells do not increase the cellular GSH level, rather it maintains the level of GSH even in the presence buthionine sulfoximine, an irreversible inhibitor of γ-glutamylcysteinesynthetase, a rate-limiting enzyme in GSH synthesis, which leads to GSH depletion and modulates the cellular redox status. As expected, exposure of DDVP leads to the decrease (~25%) decrease in cellular GSH level in WRL-68 cells, however cells pre-incubated with CeNPs did not show any decrease in GSH level when compared with untreated control cells. In fact, the level of produced GSH was more than untreated control in cells pre-incubated with CeNPs and later exposed to 50 µM concentration of DDVP. These observations suggest that CeNPs reinforces the production of cellular GSH level in cells.

Cellular reactive oxygen species are scavenged by CeNPs

As observed in **Fig. 3C,** DDVP exposure to WRL-68 cells results in the decreased production of cellular GSH level, we further examined the reactive oxygen species generation in cells. 2′,7′-dichlorodihydrofluorescein diacetate (H_2DCF-DA) were used for detection of ROS generated in cells. H_2DCF-DA dye diffuses across the cell membrane and is subsequently oxidized to membrane impermeable, highly fluorescent DCF by intracellular ROS. Cells were exposed to 200 µM concentration of DDVP with and without pre-incubation, with 50 µM CeNPs followed by incubation with H_2DCF-DA dye. The resulting ROS generated in cells were imaged under a fluorescence microscope **(Fig. 4 A - P)**. Results clearly depict some level of green fluorescence visible from untreated control cells **(Fig, 4 A – D),** which could be ascribed to a certain basic level of ROS already present in the cell cytoplasm. As expected, cells exposed to 50 µM pristine CeNPs **(Fig. 4 E – H)** also exhibited green fluorescence similar to untreated control cells, suggesting that CeNPs treatment to WRL-68 do not enhance ROS formation. However, cells exposed to DDVP exhibited intense green fluorescence signal from the cytoplasm, suggesting a very high concentration amount of ROS generation in cells **(Fig. 4 I – L)**. Interestingly, WRL-68 cells pre-incubated with CeNPs for 6 hrs followed by DDVP exposure showed a significant decrease in green fluorescence signal from cells, suggesting that the presence of CeNPs in cytoplasm have efficiently scavenged the excess ROS generated due to DDVP exposure **(Fig. 4 M – P)**. A quantitative estimate was also studied by fluorescence spectrophotometer **(Fig. 4 Q)**. Results show that 100 and 200 µM DDVP exposure leads to 167 and 211% increase in ROS generation, respectively. However WRL-68 cells pre-treated with 50 µM concentration of CeNPs before DDVP exposure exhibited a significant decrease in ROS level.

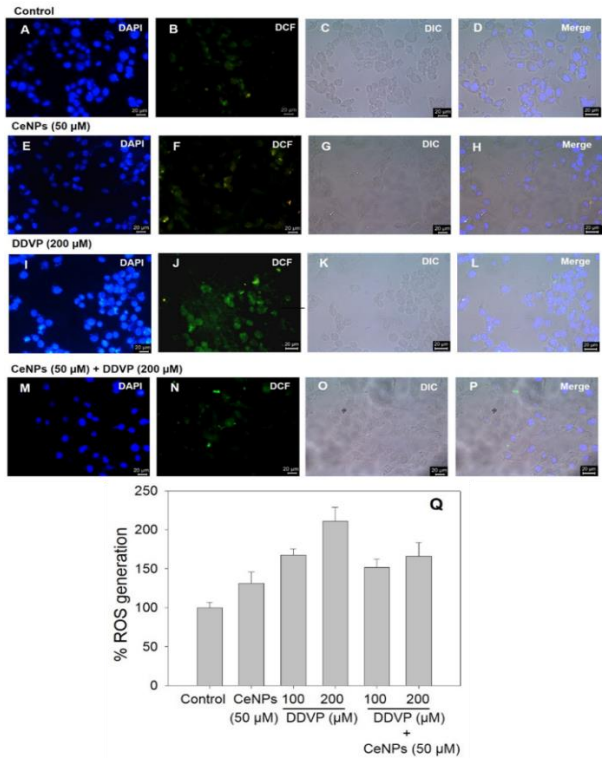

Fig. 4. CeNPs reduces the level of free radicals in cell cytoplasm induced by DDVP exposure. CeNPs untreated or pre-treated cells were exposed to DDVP followed by H_2DCFDA dye before imaged under fluorescence microscope. Untreated cells (A – D), 50 µM CeNPs treated cells (E – H), 200 µM DDVP treated cells (I – L) and 50 µM CeNPs pre-treated followed by 200 µM DDVP exposed cells (M – P) were imaged under fluorescence microscope. The ROS generation was quantified by measuring the emission intensity (Ex. 485/Em. 520 nm) of H_2DCFDA dye from cells treated with DDVP, with or without pre-treatment of CeNPs, by spectrophotometer (Q). Data expressed as SD calculated from three (n = 3) independent experiments.

CeNPs protects cells from nuclear fragmentation induced by DDVP

Nanomaterials smaller than 50 nm diameter are reported to be easily internalized in the nucleus and damage genetic materials including DNA. Further, DDVP is also reported to induce DNA damage in mammalian cells, probably decrease in cellular GSH level enable cellular genetic materials more prone to be damaged. DDVP is also known to induce DNA damage which could be attributed due to the cellular GSH depletion during DDVP detoxification, which further facilitates the susceptibility of liver cells for damage caused due to ROS generation [39]. Therefore, we next investigated the protective effect of CeNPs against the nuclear fragmentation caused by DDVP in WRL-68 cells. Estimation of nuclear fragmentation was measured by staining the cells after DDVP treatment with and without pre-incubation with CeNPs, with DAPI and imaged under fluorescence microscopy **(Fig. 5)**. Results clearly show the DDVP (100 and 200 µM) exposure leads to increase in the number of fragmented nuclei **(Fig. 5C** and **D)** when compared to untreated control cells **(Figure 5A)** and only CeNPs treated cells **(Fig. 5B).** However, cells pre-treated with CeNPs showed healthy nuclei without any fragmentation **(Fig. 5E** and **F)**. To obtain a quantitative estimation ~150 cells nuclei were counted from each treatment **(Fig. 5G).** Result depicts that 100 and 200 µM DDVP exposure leads to significant increase in fragmented nuclei, whereas, cell pre-treated with CeNPs shows less fragmented nuclei, suggesting the protective effect of nuclear fragmentation. Thus it can be concluded that CeNPs can overcome the genetic material damage caused due to the toxic effect of DDVP thereby protect mammalian cells.

SOD activity of CeNPs is not altered by interaction with DDVP

The above results suggest that CeNPs could abrogate the toxic events generated by DDVP. Several other antioxidants have been reported to be used to circumvent the toxicity of DDVP, however, very frequently molecular antioxidants react with DDVP and lose their ROS scavenging capacity [40-43]. Further, DDVP exposure also inactivates the endogenous antioxidant enzymes such as superoxide dismutase and catalase [43]. In this context, if an inorganic antioxidant could act as a suitable alternative to the molecular antioxidant, which is unreactive towards DDVP, it would be of great interest. Therefore, we next examined the chemical reaction between DDVP and CeNPs. Owing to the high surface to volume ratio, nanomaterials are expected to be very reactive, therefore it becomes furthermore important to investigate any potential interaction between CeNPs and DDVP and its effect over SOD enzyme-like activity of CeNPs. The interaction between DDVP and CeNPs were evaluated by following the UV-vis absorbance pattern and SOD activity of CeNPs physically mixed with DDVP **(Fig. 6).** CeNPs (500 µM) were incubated with different concentrations of DDVP

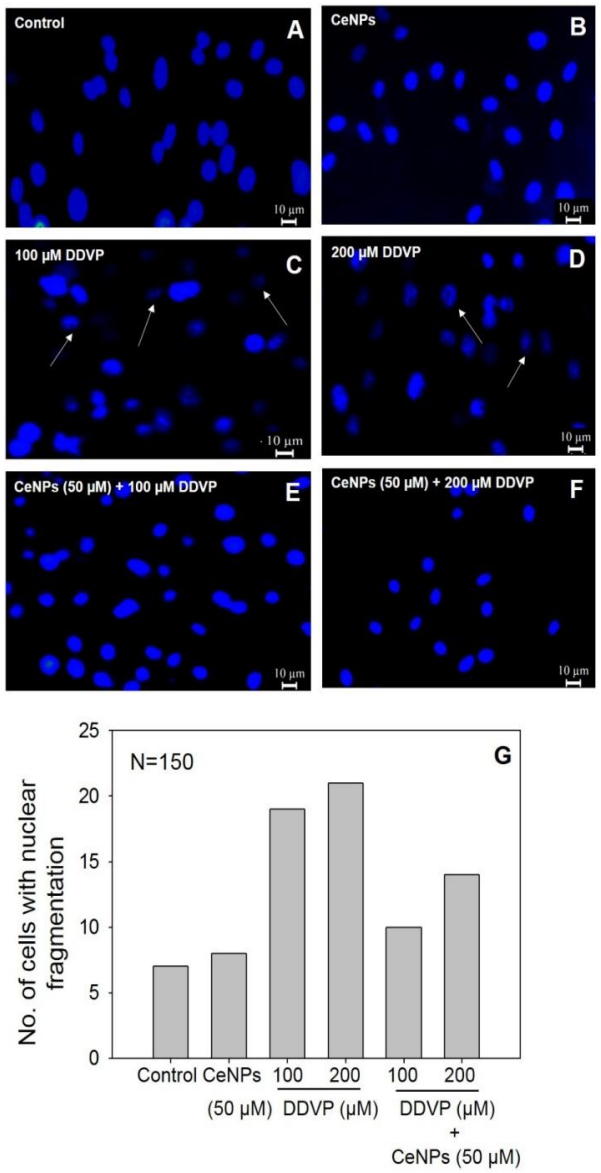

Fig. 5. CeNPs inhibit nuclear fragmentation events induced by DDVP in WRL-68 cells. Untreated (A) or CeNPs (50 µM) pre-treated (B, E & F) cells were exposed to DDVP (100, 200 µM), followed by nuclei staining with DAPI. Images were recorded by fluorescence microscope. Anti-genotoxic potential of CeNPs was quantified by counting 150 cells exposed to CeNPs, DDVP, and cells exposed to DDVP with or without pre-treatment of CeNPs (G). Data expressed as SD calculated from three (n = 3) independent experiments.

(100, 200, 500 and 1000 µM) followed by absorbance spectra measurement **(Fig. 6A).** Absorbance pattern of aqueous CeNPs (black curve) showed a clear absorbance peak at ~254 nm, characteristic to CeNPs with high +3 oxidation state surface "Ce" atoms [8]. Similarly, the aqueous solution of pure DDVP showed a broad absorbance pattern from 260 – 275 nm (red curve). The absorbance spectra of 500 µM of CeNPs mixed with lower concentrations of DDVP (100 and 200 µM) resulted in the absorbance peak matching well with the pure CeNPs, which could be due to the higher concentration of CeNPs than DDVP. Interestingly, when 500 µM CeNPs was mixed with an equimolar

concentration of DDVP, two absorbance peaks could be observed, one at 254 nm and another abroad absorbance hump ranging from 270 nm, which could be ascribed due to the CeNPs and DDVP, respectively. In another mixture containing 500 µM of CeNPs and excess (1000 µM) of DDVP clearly showed two absorbance peaks, matching well with CeNPs and DDVP. These observations suggest that CeNPs do not interact with DDVP when mixed in an aqueous suspension. Further, we also investigated the SOD-like activity of CeNPs exposed to different concentrations of DDVP **(Fig. 6B).** CeNPs (150 µM) were incubated with 100 and 200 µM of DDVP, followed by overnight incubation, the SOD-like activity of CeNPs was examined. As clearly evident from the figure that even higher concentrations of DDVP did not alter the SOD-like activity of CeNPs. As expected, DDVP alone did not show any SOD-like activity. Thus it is expected that unlike molecular antioxidants, the antioxidant activity of CeNPs would be unaltered when exposed to DDVP.

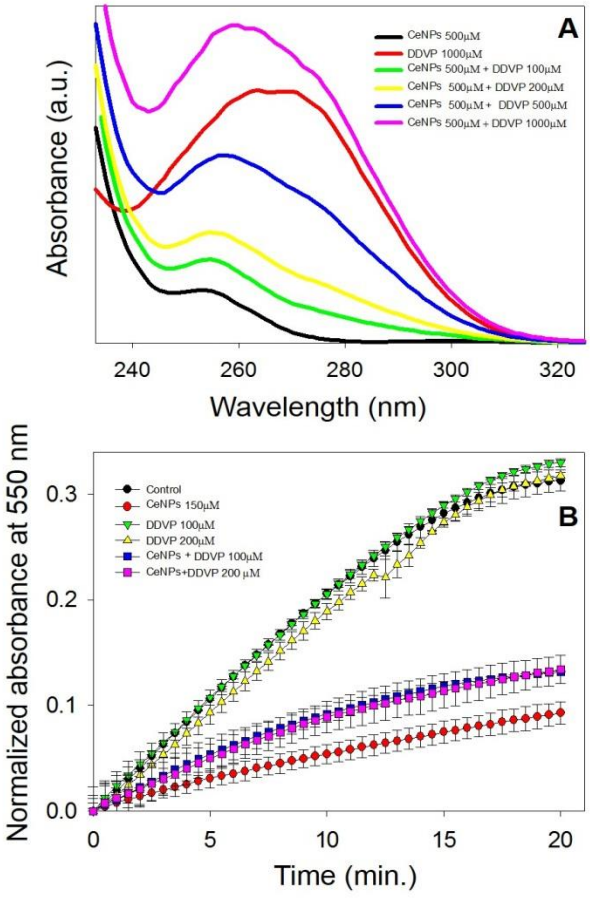

Fig. 6. DDVP do not alter the intrinsic properties of CeNPs. (A) UV-visible absorbance patterns of CeNPs (500 µM), DDVP (1000 µM) and mixture of CeNPs (500 µM) and different concentrations of DDVP (100, 200, 500, 1000 µM). (B) SOD mimetic activity of CeNPs (150 µM), DDVP (100, 200 µM) and mixture of CeNPs and different concentrations of DDVP (100, 200 µM) was followed by reduction of ferricytochrome C by superoxide spectrophotometrically at 550 nm for 20 mins using hypoxanthine/xanthine oxidase to generate superoxide radicals. Data expressed as SD calculated from three (n = 3) independent experiments.

Autocatalytic activity of CeNPs is not altered by DDVP

SOD and catalase-like activity of CeNPs are reported due to the mixed valence state of +3 and +4 in surface "Ce" atoms. Further, the easy interconversion between these oxidation states facilitates the auto-regeneration of surface atoms in CeNPs. Therefore, to investigate the auto-regenerative capability of CeNPs after the exposure of DDVP, we performed an oxidation reaction using H_2O_2. CeNPs (high +3/+4 ratio) is known to be rapidly and completely oxidized to +4 oxidation sate upon reaction with H_2O_2. During this reaction, the color of the solution changes from colorless to yellow colored within 5-10 mins **(Fig. 7, bottle 4).** Since CeNPs has auto-regenerative property, this yellow colored solution becomes colorless in about 15 days, which is suggested due to the regeneration of +3 oxidation state of surface "Ce" atoms. Phosphate exposure to CeNPs is reported to block the regenerative capability of nanoparticles due to the formation of cerium phosphate[44]. Further, cerium oxide is also shown to have high affinity towards phosphate anions. Therefore, we exposed CeNPs with DDVP for 24 hrs followed by H_2O_2 addition to the reaction **(Fig. 7, bottle 5)**. Similar to pristine CeNPs (+3) suspension, DDVP exposed CeNPs solution also turns yellow, suggesting that CeNPs (+3) do not react with DDVP. This result further supports our observation with UV-vis spectra and SOD-like activity **(Fig. 6)** pattern of CeNPs in presence and absence of DDVP. Additionally, we also followed the UV-vis absorbance pattern of CeNPs before and after exposure with DDVP and H_2O_2. As expected, aqueous CeNPs (colorless) show a clear absorbance at 254 nm **(Fig. 7, bottle-1),** however after H_2O_2 addition, this solution turns yellow and the concomitant UV-vis absorbance pattern also changes to exhibit a broad absorbance in the range of 300 – 400 nm, corresponding to CeNPs (+4) oxidation state **(Fig. 7, bottle 4).** Further, the aqueous CeNPs suspension after exposure to DDVP followed by H_2O_2 addition leads to the absorbance pattern (Figure 7, bottle 5) similar to the pristine CeNPs exposed to H_2O_2. Additionally, UV-vis pattern of CeNPs and DDVP mixture show a broad absorbance peak, which could be due to the merged signature absorbance of CeNPs (+3) and DDVP solution (bottle 3). Further, the exposure of DDVP with H_2O_2 do not produce any color change (bottle 6) suggesting that the color change is due to the oxidation of surface "Ce" atoms of CeNPs. Thus these observations suggest that CeNPs do not react with DDVP therefore, the autocatalytic activity of CeNPs is preserved.

Additionally, the interaction between CeNPs and DDVP was also examined by FTIR spectral analysis **(Fig. 7B).** CeNPs showed the distinct transmission band at ~1380 cm−1, characteristic Ce-O vibration **(Fig. 7B, black curve)** from CeO_2 [45], whereas, DDVP alone do not show any transmission band in this region **(Fig. 7B, red curve).** Interestingly, the transmission peak of Ce - O remain present in the CeNPs even after incubation with DDVP **(Fig. 7B, green curve),** suggest that there is no interaction between CeNPs and DDVP. FTIR

observation is in agreement with our above-mentioned results and clearly, depicts that there is no interaction between the CeNPs and DDVP. Zeta potential values were also recorded for CeNPs incubated with different DDVP concentration (100, 200 and 500 µM) **(Table 2).** Results show that upon exposure to DDVP, zeta potential values of CeNPs get decreased from 33.13 mV to 2.39 mV, this could be ascribed due to the electrostatic interaction of positively charged CeNPs with negatively charged phosphate groups of DDVP.

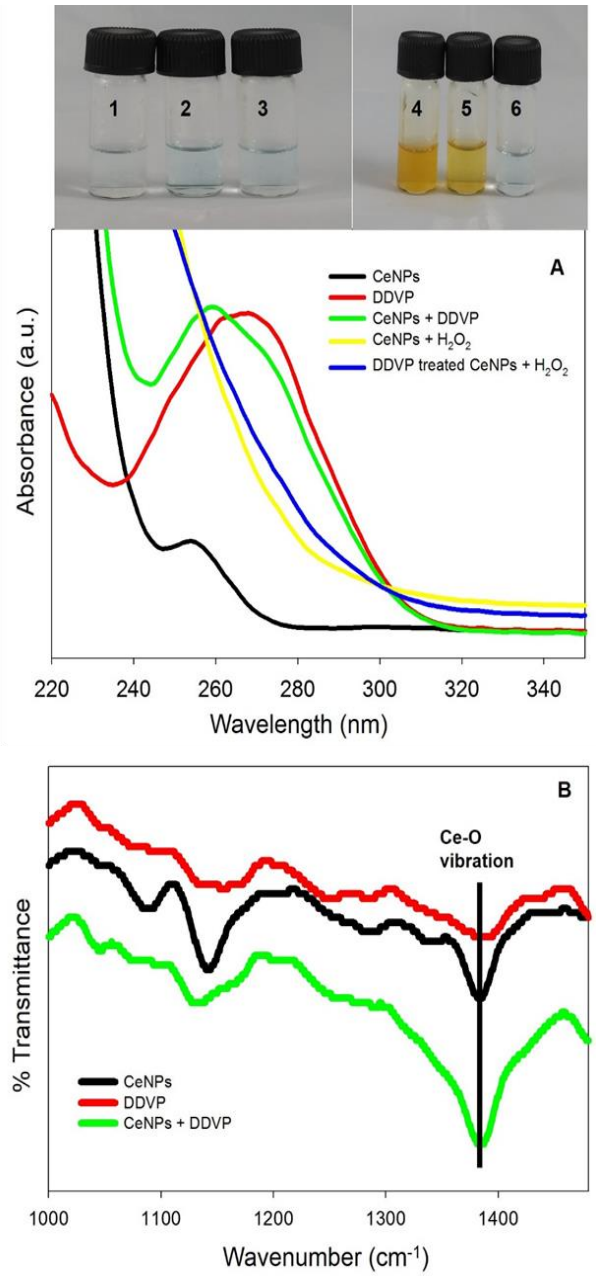

Fig. 7. (A) DDVP do not alter the autocatalytic activity of CeNPs. CeNPs were either exposed or unexposed to DDVP followed by H_2O_2 (1M) treatment and incubated for 1 hr. After the reaction the absorbance pattern was followed by UV-visible spectra measurements (A). Inset pictures of bottles show the color of aqueous suspension of CeNPs (1), DDVP (2), CeNPs exposed to DDVP (3), CeNPs exposed to H_2O_2 (4), CeNPs treated with DDVP followed by H_2O_2 exposure (5) and DDVP exposed to H_2O_2 (6). (B) CeNPs, DDVP and aqueous mixture of CeNPs and DDVP was analysed by FTIR spectroscopy.

Table 2. Zeta potential values of CeNPs suspended in different concentrations of DDVP. Data provided are average of three independent experiments with standard deviation.

Nanoparticle suspension	Zeta potential (mV)
CeNPs (4mM)	33.13 ± 2.19
CeNPs (4mM)+ DDVP 100µM	2.39 ± 0.38
CeNPs (4mM)+ DDVP 200µM	3.85 ± 1.19
CeNPs (4mM)+ DDVP 500µM	3.08 ± 1.34

Conclusion

CeNPs are a unique class of inorganic nanozyme, which exhibit redox-state dependent biological antioxidant enzyme-like properties. These properties are fundamental to several applications shown with CeNPs. The results of the presented work reveal that CeNPs could potentially abrogate the toxic effects of DDVP in a normal liver cell culture model system. The rapid internalization and nearly homogeneous cellular distribution of CeNPs, shown by us and others, could be one of the major reasons to overcome the toxicity generated by reactive oxygen and nitrogen species in DDVP exposed cells. In this work, using several test methods, we have shown that the cell death caused by DDVP exposure can be prevented if cells are pre-exposed with CeNPs. Further, the nuclear fragmentation events could also be avoided with the use of CeNPs. There can be two ways for CeNPs to protect the cells from the DDVP, *first*: the antioxidant role of CeNPs itself, and *second*: CeNPs induce the high expression of GSH in WRL-68 cells. We have also shown that PEGylated CeNPs oversee the expression of antioxidant enzymes in a normal skin cell culture model but the level of GSH is unaltered. However, in WRL-68 cells (this study) the GSH level is increased upon CeNPs exposure suggesting that the mechanism of protection of CeNPs in different cells/tissues are different. This observation becomes important in the view of high concentration of GSH needed in the liver cells (~7mM), probably maximum than all other cell types of the body [46]. It has been shown that mice lacking glutamate cysteine ligase, essential for GSH synthesis, die within < 30 days of birth due to the absence of liver GSH synthesis [47]. DDVP is known to exhibit non-specific interaction with key biomolecules and antioxidant enzymes of the cells/tissues. It is also common that the antioxidant molecule irreversibly binds with the toxicants thereby reduce their toxicity. However, such contrivance may not be effective in long term. Therefore, in order to scout the possible mechanism, we also explored any chemical interaction between CeNPs and DDVP using several characterization techniques. Although it has been reported that CeNPs irreversibly react with phosphate anions, we did not find any chemical interaction between CeNPs and DDVP suggesting that use of CeNPs as an antioxidant to abrogate the effects of DDVP would be an ideal system. Further, more in-depth studies are required to establish the exact molecular mechanism occurring

during the use of CeNPs as an antioxidant to revoke the toxicity induced by DDVP. The cytoprotective effect of CeNPs can also be extended to avoid the noxious consequences of other commercially available pesticides.

Acknowledgement

The financial assistance for the Centre for Nanotechnology Research and Applications (CENTRA) by The Gujarat Institute for Chemical Technology (GICT) is gratefully acknowledged. Dr Sanjay Singh thank to Department of Science and Technology - Science and Engineering Research Board (SERB) (Grant No.: ILS/SERB/2015-16/01) for providing funding under the scheme of Start-Up Research Grant (Young Scientists) in Life Sciences. This manuscript carries a DBLS communication number DBLS - 083.

References

1. W.S. Kuo, Y.T. Chang, K.C. Cho, K.C. Chiu, C.H. Lien, C.S. Yeh, S.J. Chen, Gold nanomaterials conjugated with indocyanine green for dual-modality photodynamic and photothermal therapy, Biomaterials, 33 (2012) 3270-3278.
2. A. Jhaveri, P. Deshpande, V. Torchilin, Stimuli-sensitive nanopreparations for combination cancer therapy, J Control Release, 190 (2014) 352-370.
3. M.J. Akhtar, M. Ahamed, H.A. Alhadlaq, S.A. Alrokayan, S. Kumar, Targeted anticancer therapy: overexpressed receptors and nanotechnology, Clinica chimica acta; international journal of clinical chemistry, 436 (2014) 78-92.
4. M.S. Muthu, D.T. Leong, L. Mei, S.S. Feng, Nanotheranostics - application and further development of nanomedicine strategies for advanced theranostics, Theranostics, 4 (2014) 660-677.
5. S. Singh, Cerium oxide based nanozymes: Redox phenomenon at biointerfaces, Biointerphases, 11 (2016) 04B202.
6. A.S. Karakoti, N.A. Monteiro-Riviere, R. Aggarwal, J.P. Davis, R.J. Narayan, W.T. Self, J. McGinnis, S. Seal, Nanoceria as Antioxidant: Synthesis and Biomedical Applications, Jom (1989), 60 (2008) 33-37.
7. J. Chen, S. Patil, S. Seal, J.F. McGinnis, Rare earth nanoparticles prevent retinal degeneration induced by intracellular peroxides, Nature nanotechnology, 1 (2006) 142-150.
8. R. Singh, S. Singh, Role of phosphate on stability and catalase mimetic activity of cerium oxide nanoparticles, Colloids and surfaces, 132 (2015) 78-84.
9. J.M. Dowding, T. Dosani, A. Kumar, S. Seal, W.T. Self, Cerium oxide nanoparticles scavenge nitric oxide radical (NO), Chemical communications (Cambridge, England), 48 (2012) 4896-4898.
10. J.M. Dowding, S. Seal, W.T. Self, Cerium oxide nanoparticles accelerate the decay of peroxynitrite (ONOO(-)), Drug delivery and translational research, 3 (2013) 375-379.
11. E.G. Heckert, A.S. Karakoti, S. Seal, W.T. Self, The role of cerium redox state in the SOD mimetic activity of nanoceria, Biomaterials, 29 (2008) 2705-2709.
12. T. Pirmohamed, J.M. Dowding, S. Singh, B. Wasserman, E. Heckert, A.S. Karakoti, J.E. King, S. Seal, W.T. Self, Nanoceria exhibit redox state-dependent catalase mimetic activity, Chemical communications (Cambridge, England), 46 (2010) 2736-2738.
13. C. Korsvik, S. Patil, S. Seal, W.T. Self, Superoxide dismutase mimetic properties exhibited by vacancy engineered ceria nanoparticles, Chemical communications (Cambridge, England), DOI (2007) 1056-1058.
14. Y. Li, X. He, J.J. Yin, Y. Ma, P. Zhang, J. Li, Y. Ding, J. Zhang, Y. Zhao, Z. Chai, Z. Zhang, Acquired superoxide-scavenging ability of ceria nanoparticles, Angewandte Chemie (International ed, 54 (2015) 1832-1835.
15. S. Singh, A. Kumar, A. Karakoti, S. Seal, W.T. Self, Unveiling the mechanism of uptake and sub-cellular distribution of cerium oxide nanoparticles, Molecular bioSystems, 6 (2010) 1813-1820.
16. A.Y. Estevez, J.S. Erlichman, The potential of cerium oxide nanoparticles (nanoceria) for neurodegenerative disease therapy, Nanomedicine (London, England), 9 (2014) 1437-1440.
17. R. Singh, A.S. Karakoti, W. Self, S. Seal, S. Singh, Redox-Sensitive Cerium Oxide Nanoparticles Protect Human Keratinocytes from Oxidative Stress Induced by Glutathione Depletion, Langmuir, 32 (2016) 12202-12211.
18. B.C. Nelson, M.E. Johnson, M.L. Walker, K.R. Riley, C.M. Sims, Antioxidant Cerium Oxide Nanoparticles in Biology and Medicine, Antioxidants (Basel, Switzerland), 5 (2016).
19. C. Xu, X. Qu, Cerium oxide nanoparticle: a remarkably versatile rare earth nanomaterial for biological applications, NPG Asia Mater, 6 (2014) e90.
20. O. Blessing, I.C. Grace, Acute Toxicity of the Pesticides, Dichlorvos and Lindane against the African air-breathing catfish, Heterobranchus longifilis, Valenciennes, 1840 (Siluriformes: Clariidae), Recent patents on biotechnology.
21. S. Agarwal, B. Chaudhary, R. Bist, Protective propensity of bacoside A and bromelain on renal cholinesterases, gamma-Aminobutyric acid and serotonin level of Mus musculus intoxicated with dichlorvos, Chemico-biological interactions, 261 (2017) 139-144.
22. W.Y. Wani, R.J. Kandimalla, D.R. Sharma, A. Kaushal, A. Ruban, A. Sunkaria, J. Vallamkondu, A. Chiarugi, P.H. Reddy, K.D. Gill, Cell cycle activation in p21 dependent pathway: An alternative mechanism of organophosphate induced dopaminergic neurodegeneration, Biochimica et biophysica acta.
23. B.K. Binukumar, N. Gupta, A. Sunkaria, R. Kandimalla, W.Y. Wani, D.R. Sharma, A. Bal, K.D. Gill, Protective efficacy of coenzyme Q10 against DDVP-induced cognitive impairments and neurodegeneration in rats, Neurotoxicity research, 21 (2012) 345-357.
24. A. Moretto, M. Lotti, P.S. Spencer, In vivo and in vitro regional differential sensitivity of neuropathy target esterase to di-n-butyl-2,2-dichlorovinyl phosphate, Archives of toxicology, 63 (1989) 469-473.
25. T.C. Hoang, G.M. Rand, Acute toxicity and risk assessment of permethrin, naled, and dichlorvos to larval butterflies via ingestion of contaminated foliage, Chemosphere, 120 (2015) 714-721.
26. I. Ben Salem, M. Boussabbeh, H. Bacha, S. Abid, Dichlorvos-induced toxicity in HCT116 cells: involvement of oxidative stress and apoptosis, Pesticide biochemistry and physiology, 119 (2015) 62-66.
27. T.M. Bui-Nguyen, W.E. Dennis, D.A. Jackson, J.D. Stallings, J.A. Lewis, Detection of dichlorvos adducts in a hepatocyte cell line, Journal of proteome research, 13 (2014) 3583-3595.
28. B.K. Binukumar, A. Bal, R. Kandimalla, A. Sunkaria, K.D. Gill, Mitochondrial energy metabolism impairment and liver dysfunction following chronic exposure to dichlorvos, Toxicology, 270 (2010) 77-84.
29. S. Patel, M. Bajpayee, A.K. Pandey, D. Parmar, A. Dhawan, In vitro induction of cytotoxicity and DNA strand breaks in CHO cells exposed to cypermethrin, pendimethalin and dichlorvos, Toxicol In Vitro, 21 (2007) 1409-1418.
30. S. Eroglu, D. Pandir, F.G. Uzun, H. Bas, Protective role of vitamins C and E in dichlorvos-induced oxidative stress in human erythrocytes in vitro, Biological research, 46 (2013) 33-38.
31. L. Audegond, D. Catez, P. Foulhoux, R. Fournex, C. Le Rumeur, M. L'Hotellier, J.P. Stepniewski, Potentiation of deltamethrin toxicity by organophosphorus insecticides, Journal de toxicologie clinique et experimentale, 9 (1989) 163-176.
32. A.S. Karakoti, S. Singh, A. Kumar, M. Malinska, S.V. Kuchibhatla, K. Wozniak, W.T. Self, S. Seal, PEGylated nanoceria as radical scavenger with tunable redox chemistry, Journal of the American Chemical Society, 131 (2009) 14144-14145.
33. H. Suzuki, T. Toyooka, Y. Ibuki, Simple and easy method to evaluate uptake potential of nanoparticles in mammalian cells using a flow cytometric light scatter analysis, Environmental science & technology, 41 (2007) 3018-3024.
34. T. Mosmann, Rapid colorimetric assay for cellular growth and survival: application to proliferation and cytotoxicity assays, Journal of immunological methods, 65 (1983) 55-63.
35. M.M. Yallapu, N. Chauhan, S.F. Othman, V. Khalilzad-Sharghi, M.C. Ebeling, S. Khan, M. Jaggi, S.C. Chauhan, Implications of protein corona on physico-chemical and biological properties of magnetic nanoparticles, Biomaterials, 46 (2015) 1-12.

36. D. Pozzi, G. Caracciolo, A.L. Capriotti, C. Cavaliere, G. La Barbera, T.J. Anchordoquy, A. Lagana, Surface chemistry and serum type both determine the nanoparticle-protein corona, Journal of proteomics, 119 (2015) 209-217.
37. Z. Ji, X. Jin, S. George, T. Xia, H. Meng, X. Wang, E. Suarez, H. Zhang, E.M. Hoek, H. Godwin, A.E. Nel, J.I. Zink, Dispersion and stability optimization of TiO2 nanoparticles in cell culture media, Environmental science & technology, 44 (2010) 7309-7314.
38. G. Repetto, A. del Peso, J.L. Zurita, Neutral red uptake assay for the estimation of cell viability/cytotoxicity, Nature protocols, 3 (2008) 1125-1131.
39. T. Yamano, Dissociation of DDVP-induced DNA strand breaks from oxidative damage in isolated rat hepatocytes, Toxicology, 108 (1996) 49-56.
40. G.O. Ochigbo, A.B. Saba, A.A. Oyagbemi, T.O. Omobowale, E.R. Asenuga, Polyphenol-rich fraction of Parquetina nigrescens mitigates dichlorvos-induced neurotoxicity and apoptosis, Journal of Ayurveda and integrative medicine.
41. H. Alp, N. Pinar, R. Dokuyucu, M. Sahan, C. Oruc, I. Kaplan, S. Senol, A.B. Ceyran, Protective Effects of Intralipid and Caffeic Acid Phenethyl Ester (CAPE) on Hepatotoxicity and Pancreatic Injury Caused by Dichlorvos in Rats, Biochemical genetics, 54 (2016) 803-815.
42. X.C. Huo, S.S. Liu, J. Zhang, J. Zhang, Characterizing the toxicity interaction of the binary mixture between DMSO and pesticide by the multi-effect residual analysis (MERA), Huan jing ke xue= Huanjing kexue, 34 (2013) 257-262.
43. M.Y. Xu, P. Wang, Y.J. Sun, H.P. Wang, Y.J. Liang, L. Zhu, Y.J. Wu, Redox status in liver of rats following subchronic exposure to the combination of low dose dichlorvos and deltamethrin, Pesticide biochemistry and physiology, 124 (2015) 60-65.
44. S. Singh, T. Dosani, A.S. Karakoti, A. Kumar, S. Seal, W.T. Self, A phosphate-dependent shift in redox state of cerium oxide nanoparticles and its effects on catalytic properties, Biomaterials, 32 (2011) 6745-6753.
45. B. Yan, H. Zhu, Controlled synthesis of CeO2 nanoparticles using novel amphiphilic cerium complex precursors, Journal of Nanoparticle Research, 10 (2008) 1279-1285.
46. N. Kaplowitz, The importance and regulation of hepatic glutathione, The Yale journal of biology and medicine, 54 (1981) 497-502.
47. H. Sies, Glutathione and its role in cellular functions, Free radical biology & medicine, 27 (1999) 916-921.

